Human Pathology (2019) **84**, 81–91

ELSEVIER

Human PATHOLOGY

www.elsevier.com/locate/humpath

Original contribution

Nuclear immunoreactivity of BLM-s, a proapoptotic BCL-2 family member, is specifically detected in salivary adenoid cystic carcinoma☆,☆☆

Mu-Shiun Tsai MD[a,b], Min-Shu Hsieh MD, PhD[a,c], Hsin-Yi Huang MD, PhD[c], Pei-Hsin Huang MD[a,c,*]

[a]*Graduate Institute of Pathology, College of Medicine, National Taiwan University, Taipei 100, Taiwan, ROC*
[b]*Department of Pathology, Landseed Hospital, Taoyuan 324, Taiwan, ROC*
[c]*Department of Pathology, National Taiwan University Hospital, Taipei 100, Taiwan, ROC*

Received 2 June 2018; revised 12 September 2018; accepted 14 September 2018

Keywords:
Salivary adenoid cystic carcinoma (ACC);
BLM-s;
C-KIT;
Immunohistochemistry;
MYB (*MYBL*) FISH

Summary Tumor cells frequently evade apoptosis triggered by cellular stress via aberrant regulation of the BCL-2 family members, which are key players in regulating cell death under physiological and pathological situations. Previously, we have identified a novel BH3-only protein of the BCL-2 family, BLM-s (BCL-2–like molecule, short form), that modulates apoptosis of postmitotic immature neurons during corticohistogenesis. Whether BLM-s expression correlates with any subtype of human tumors has not been investigated. Here, via BLM-s immunohistochemistry performed in various kinds of human tumors, we demonstrate that BLM-s is specifically expressed in tumors derived from salivary gland (specificity, 0.76 [95% confidence interval, or CI], 0.65-0.85]; sensitivity, 1 [95% CI, 0.99-1]). Stratification of BLM-s immunointensity and its subcellular localization in correlation with salivary gland tumor subtype shows a statistically significant increase in proportion and in intensity of nuclear staining for adenoid cystic carcinoma (ACC; specificity, 0.92 [95% CI, 0.88-0.95]; sensitivity, 0.82 [95% CI, 0.66-0.92]), a locally aggressive head and neck malignancy. Comparison among salivary ACC in correlation with *MYB/MYBL* fluorescence in situ hybridization, c-KIT immunohistochemistry, and BLM-s immunohistochemistry shows that BLM-s' nuclear immunoreactivity has lower false-negative detection rate (18.5% compared with 26.3% [*MYB/MYBL* fluorescence in situ hybridization] and 34.2% [c-KIT], respectively). Intriguingly, ACC derived from other cell origins such as breast shows negative BLM-s immunoreactivity. We thus propose that nuclear localization of BLM-s detected by immunohistochemistry could be potentially used as an ancillary diagnostic marker for ACC originating from the salivary gland, especially when the biopsy specimen is small with an unknown tumor origin.

1. Introduction

Apoptosis is one of the key tumor-suppression mechanisms and is mainly regulated by the BCL-2 family [1]. Cancer cells frequently dysregulate BCL-2 family members to evade apoptosis triggered by hypoxia and genomic instability [2].

☆ Competing interests: We declare that we have no conflict of interest.
☆☆ Funding/Support: This work was supported by a grant from the Ministry of Science and Technology, ROC, to P.-H. H. (MOST104-2320-B-002-020-MY3).
* Corresponding author at: Graduate Institute of Pathology, College of Medicine, National Taiwan University, Taipei 100, Taiwan, ROC.
E-mail address: phhuang@ntu.edu.tw (P. -H. Huang).

https://doi.org/10.1016/j.humpath.2018.09.005
0046-8177/

Table 1 BLM-s immunohistochemistry in various types of human tumors (some paired with normal tissues)

Organ	Diagnosis	Case no.	Negative (%)	Positive (%)	
				Cytoplasmic	Nuclear
Brain	Normal	12	12 (100)	0 (0)	0 (0)
	Low-grade astrocytoma	6	6 (100)	0 (0)	0 (0)
	Pilocytic astrocytoma	4	4 (100)	0 (0)	0 (0)
	Anaplastic astrocytoma	6	6 (100)	0 (0)	0 (0)
	Glioblastoma	5	5 (100)	0 (0)	0 (0)
	Medulloblastoma	3	3 (100)	0 (0)	0 (0)
	Central neurocytoma	2	2 (100)	0 (0)	0 (0)
	Dysembryoplastic neuroepithelial tumor	1	1 (100)	0 (0)	0 (0)
	Meningioma	12	12 (100)	0 (0)	0 (0)
Lung	Normal	12	12 (100)	0 (0)	0 (0)
	Squamous cell carcinoma	15	15 (100)	0 (0)	0 (0)
	Adenocarcinoma	18	18 (100)	0 (0)	0 (0)
	Mucoepidermoid carcinoma	2	2 (100)	0 (0)	0 (0)
	Small cell carcinoma	8	8 (100)	0 (0)	0 (0)
Esophagus	Normal	10	10 (100)	0 (0)	0 (0)
	Squamous cell carcinoma	10	10 (100)	0 (0)	0 (0)
Stomach	Normal	12	12 (100)	0 (0)	0 (0)
	Adenocarinoma, intestinal type	10	10 (100)	0 (0)	0 (0)
	Adenocarcinoma, diffuse type	6	6 (100)	0 (0)	0 (0)
Colon	Normal	16	16 (100)	0 (0)	0 (0)
	Adenocarcinoma	21	21 (100)	0 (0)	0 (0)
Salivary gland	Normal	8	2 (25)	6 (75) [a]	0 (0)
	Post irradiated	4	0 (0)	4 (100) [b]	0 (0)
	Tumor [c]	299	115 (38.5)	144 (48.2)	40 (13.4)
Gallbladder	Normal	2	2 (100)	0 (0)	0 (0)
	Adenocarcinoma	2	2 (100)	0 (0)	0 (0)
Liver	Normal	12	12 (100)	0 (0)	0 (0)
	Hepatocellular carcinoma	18	18 (100)	0 (0)	0 (0)
	Intrahepatic cholangiocarcinoma	6	6 (100)	0 (0)	0 (0)
Kidney	Normal	11	11 (100)	0 (0)	0 (0)
	Clear cell renal cell carcinoma	12	12 (100)	0 (0)	0 (0)
	Chromophobe renal cell carcinoma	8	8 (100)	0 (0)	0 (0)
	Papillary renal cell carcinoma	1	1 (100)	0 (0)	0 (0)
	Renal cell carcinoma, unclassified	1	1 (100)	0 (0)	0 (0)
	Invasive urothelial carcinoma	12	12 (100)	0 (0)	0 (0)
Adrenal gland	Normal	9	9 (100)	0 (0)	0 (0)
	Pheochromocytoma	14	14 (100)	0 (0)	0 (0)
	Neuroblastoma	5	5 (100)	0 (0)	0 (0)
Parathyroid	Hyperplasia	2	2 (100)	0 (0)	0 (0)
Breast	Normal	16	16 (100)	0 (0)	0 (0)
	Invasive ductal carcinoma, no special type	25	25 (100)	0 (0)	0 (0)
	Invasive lobular carcinoma	8	8 (100)	0 (0)	0 (0)
	Mucinous carcinoma	2	2 (100)	0 (0)	0 (0)
	Medullary carcinoma	2	2 (100)	0 (0)	0 (0)
	ACC	3	3 (100)	0 (0)	0 (0)
	Metaplastic carcinoma	2	2 (100)	0 (0)	0 (0)
Eye	Normal	1	1 (100)	0 (0)	0 (0)
	Malignant melanoma	1	1 (100)	0 (0)	0 (0)
Skin	Non-neoplastic	15	15 (100)	0 (0)	0 (0)
	Chondroid syringoma	5	5 (100)	0 (0)	0 (0)
Soft tissue	Paraganglioma	8	8 (100)	0 (0)	0 (0)
	Olfactory neuroblastoma	2	2 (100)	0 (0)	0 (0)
	Ewing sarcoma	2	2 (100)	0 (0)	0 (0)

[a] Cytoplasmic stain in striated ductal epithelia.
[b] More intense cytoplasmic stain than nonirradiated salivary gland.
[c] Salivary gland tumors listed in Table 2.

For example, overexpression of prosurvival BCL2 family members has been reported in lung cancers [3] and glioma [4]. Inactivation or down-regulation of proapoptotic BAX is observed in ovarian cancer [5], prostate cancer [6], and hematopoietic malignancies [7]. Genomic loss of BH3-only proapoptotic BIM or PUMA was reported in lymphoma [8] and renal cell carcinoma [9].

We have previously identified a proapoptotic BH3-only member of the BCL-2 family, BLM-s (*B*CL-2–*l*ike *m*olecule, *s*hort form), which modulates apoptosis of postmitotic immature migratory neurons in response to DNA double-strand breaks during murine neocortical development [10]. Whether BLM-s plays a role in the pathophysiology of human diseases remains unexplored. Overexpression of the human homolog of *BLM-s*

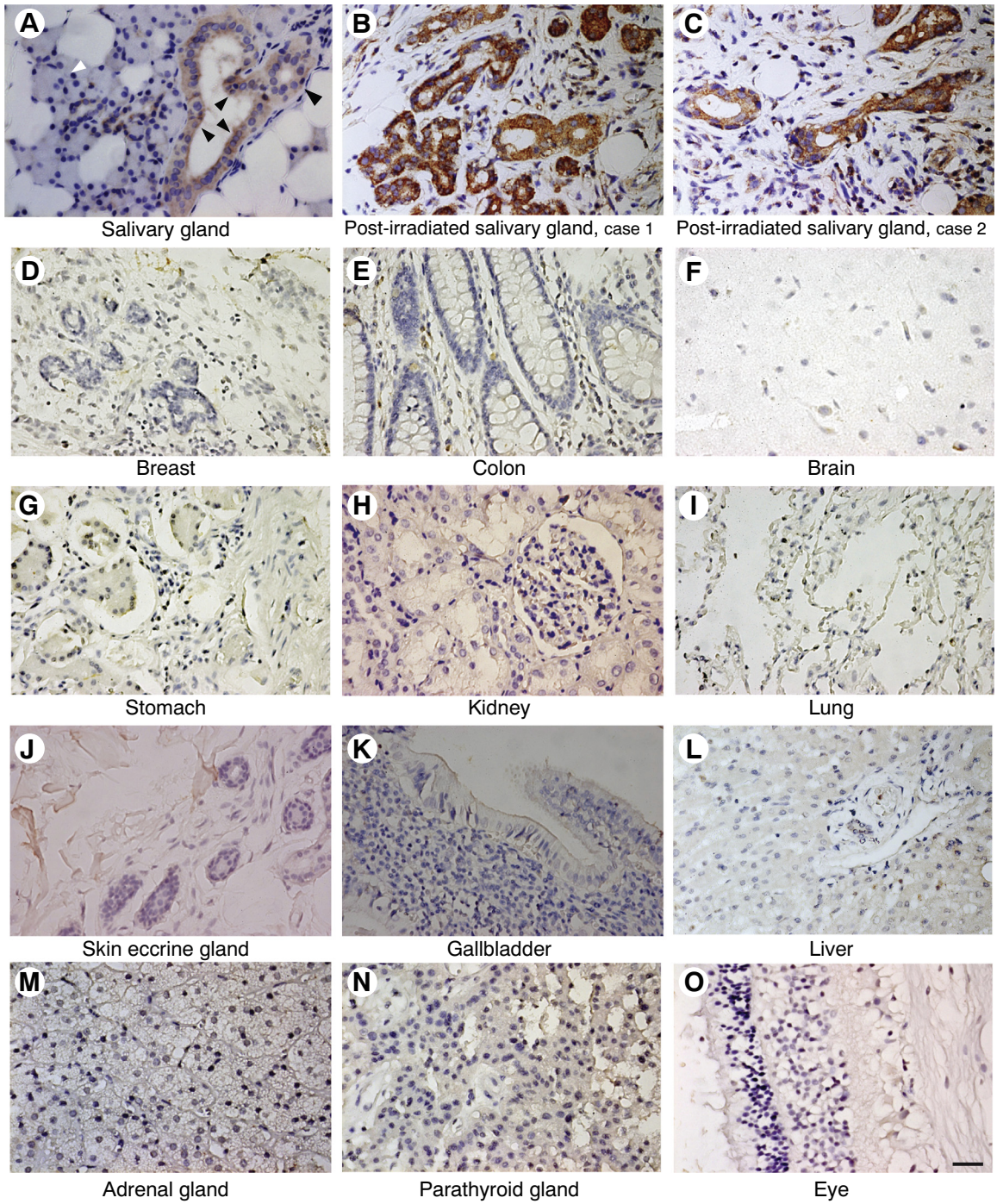

Fig. 1 BLM-s immunohistochemistry in normal human tissues. BLM-s is detected in salivary gland, normal (A) or postirradiated (B and C), and not detectable in other organs (D-O). Noticeably, BLM-s immunointensity is much increased in ductal epithelia of salivary glands receiving irradiation treatment, which is evidenced by glandular atrophy and stromal fibrosis with lymphocyte infiltrate. Black arrowheads, striated ductal epithelia; white arrowhead, acini. Scale bar, 50 μm.

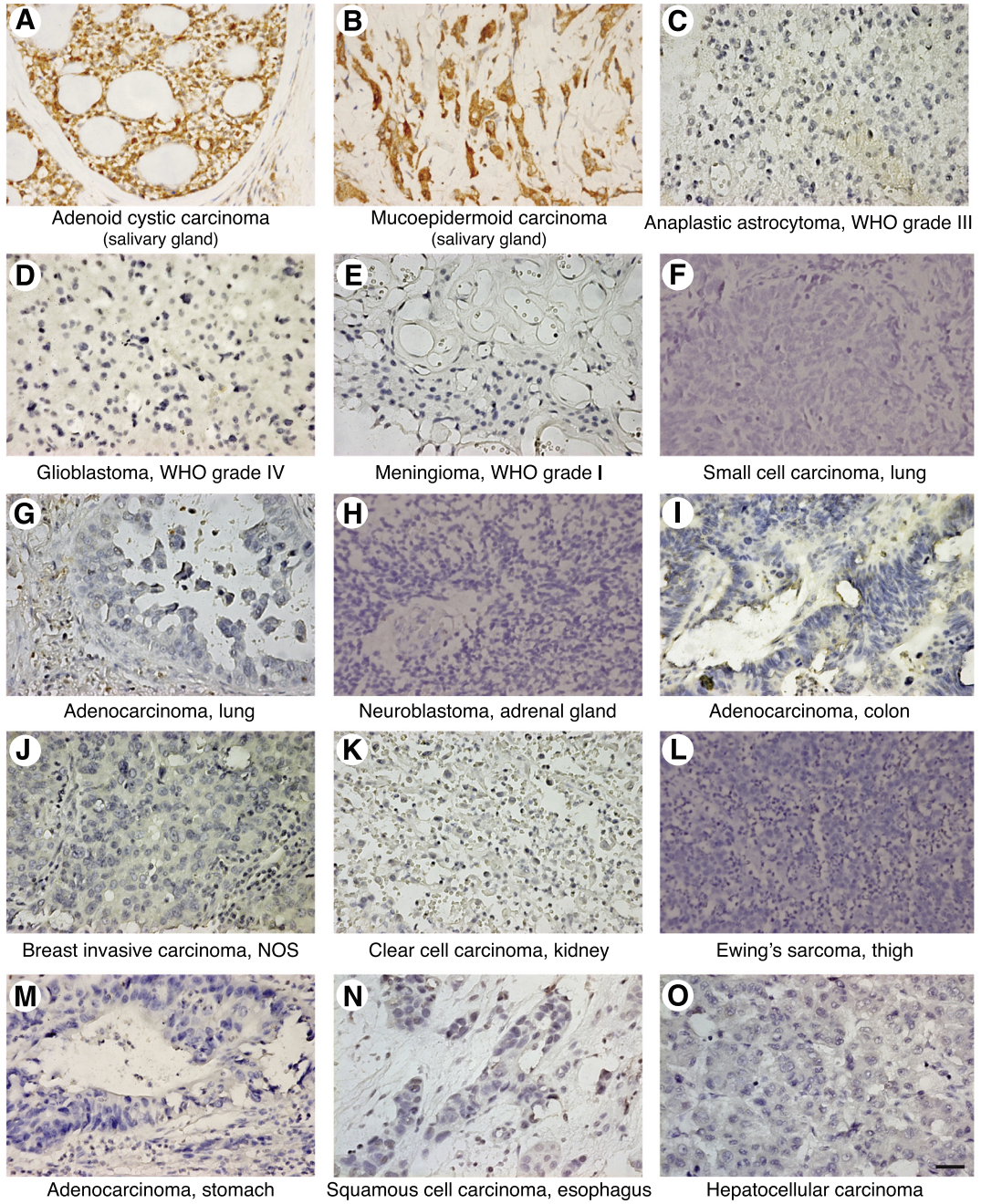
A
Adenoid cystic carcinoma
(salivary gland)
B
Mucoepidermoid carcinoma
(salivary gland)
C
Anaplastic astrocytoma, WHO grade III
D
Glioblastoma, WHO grade IV
E
Meningioma, WHO grade I
F
Small cell carcinoma, lung
G
Adenocarcinoma, lung
H
Neuroblastoma, adrenal gland
I
Adenocarcinoma, colon
J
Breast invasive carcinoma, NOS
K
Clear cell carcinoma, kidney
L
Ewing's sarcoma, thigh
M
Adenocarcinoma, stomach
N
Squamous cell carcinoma, esophagus
O
Hepatocellular carcinoma

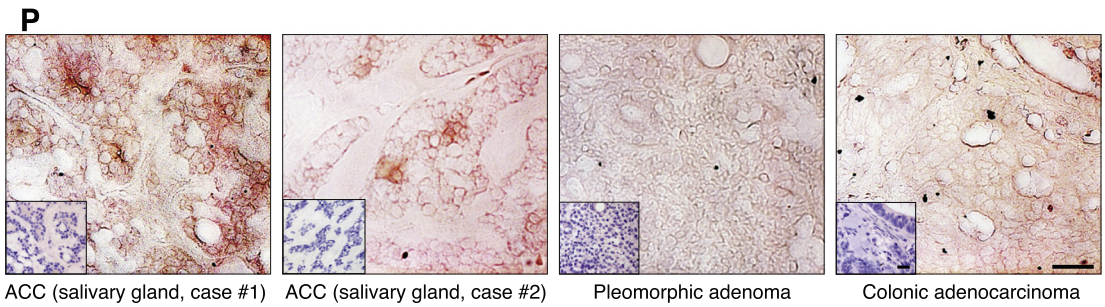
P
ACC (salivary gland, case #1)
ACC (salivary gland, case #2)
Pleomorphic adenoma
Colonic adenocarcinoma

isoform—*CCDC132* gene (also known as *BLM-l* [10], *mVPS50* [11], *Syndetin* [12], or *VPS54L* [13])—has been reported in T cells in atopic dermatitis [14]. However, whether BLM-s participates in tumor formation has not been investigated.

In this report, we have used immunohistochemistry to investigate the expression of BLM-s in various kinds of human tumors. Particularly, BLM-s' nuclear immunoreactivity is highly correlated with salivary adenoid cystic carcinoma (ACC), one of the most common malignancies of salivary gland. Salivary ACC accounts for approximately 1% of all head and neck malignancies with a tendency for perineural invasion and multiple local recurrences [15,16]. The pathological feature of ACC is basaloid cells arranged in 3 main architectural patterns: tubular, cribriform, or solid. Similar ACC histologic feature could be observed in other head and neck tumors, including cellular pleomorphic adenoma, basaloid squamous cell carcinoma, neuroendocrine carcinoma, and small blue round tumors. Therefore, ancillary immunohistochemistry or other genetic tools are required for diagnosis. Recently, reclassification of salivary gland tumors by tumor subtype-specific fusion oncogenes suggests that most salivary ACCs are associated with t(6;9)(q22-23;p23-34) translocation that results in *MYB-NFIB*–fused gene [17]. Here, BLM-s immunohistochemistry is compared with MYB/MYBL fluorescence in situ hybridization (FISH) in correlation with the diagnosis of salivary ACC.

2. Materials and methods

2.1. Case selection

All human tissue samples were obtained from the Department of Pathology, National Taiwan University Hospital (NTUH), from 1996 to 2014 with approved written informed consent by the patients and under the approval of NTUH Research Ethics Committee (registered under NTUH Research Ethics Committee Number: 201412108RIND). All cases included in this study were reviewed and diagnosed independently by at least 2 pathologists at NTUH. Cases of formalin-fixed, paraffin-embedded tumor tissues of different organs paired with normal tissue were randomly retrieved from the archives and selected for sectioning and immunohistochemistry. For pilot BLM-s' immunohistochemistry screening, cases of formalin-fixed, paraffin-embedded tumor tissues of different organs paired with normal tissue were randomly retrieved from the archives (numbers ranging from 2 to 12). For those with positive BLM-s immunoreactivity, more than 100 cases were retrieved for immunohistochemistry and/or FISH.

2.2. Antibodies

Polyclonal chicken antimouse BLM-s antibody and polyclonal rabbit anti–BLM-l antibody were house generated [10], and the feasibility for usage in human tissues by immunohistochemistry is described in Supplementary Fig. S1. Anti-CCDC132 (human homolog of mouse BLM-l) antibody (Santa Cruz Biotech, Dallas, TX), antihuman c-KIT antibody (Sigma-Aldrich, St. Louis, MO), and anti-SNAIL/SLUG antibody (Abcam, Cambridge, United Kingdom) were commercially purchased.

2.3. Immunohistochemistry and RNA in situ hybridization in paraffin sections

Paraffin-embedded, 5-μm-thick sections were deparaffinized and rehydrated. For immunohistochemistry, antigen retrieval was performed through microwaving in 10 mM citrate sodium (pH 6.0). After being blocked with 5% goat serum in Tris-buffered solution (TBS), the sections were incubated with primary antibody (including anti–BLM-s, 1:50 dilution; anti-CCDC132, 1:300 dilution; anti-c-KIT, 1:50 dilution, anti-SNAIL+SLUG, 1:100 dilution) overnight at 4°C. After several washes with TBS, the sections were incubated with biotin-labeled secondary antibody (1:200 dilution; Vector Laboratories, Burlingame, CA) for 1 hour at room temperature, followed by amplification with avidin-biotin complex with avidin-conjugated peroxidase (ScyTek Laboratories, Logan, UT) and colorization with 3,3′-diaminobenzidine (Vector Laboratories). For RNA in situ hybridization, a *BLM-s* riboprobe composed of sequences corresponding to human homolog *CCDC132* nucleotide 2528-3005 (accession number NM_017667) was synthesized with digoxigenin-labeled dUTP (Roche, Basel, Switzerland) and used as described before [18]. The postwashed hybridized signal was immunodetected by antidigoxigenin AP antibody (Roche) and color developed by HighDef red IHC chromogen (Enzo Life Sciences, Farmingdale, NY).

Fig. 2 BLM-s is specifically expressed in salivary gland neoplasms. A, Representative BLM-s immunoreactivity in salivary gland ACC. Noticeably, strong nuclear staining of BLM-s is seen in most tumor cells of ACC. B, Cytoplasmic BLM-s immunoreactivity mixed with some nuclear staining pattern is seen in some cases of salivary mucoepidermoid carcinoma. C-O, BLM-s immunoreactivity is not detected in other nonsalivary tumors, as representatively shown in anaplastic astrocytoma, World Health Organization (WHO) grade III (C), glioblastoma, WHO grade IV (D), meningioma, WHO grade I (E), lung small cell carcinoma (F), lung adenocarcinoma (G), adrenal gland neuroblastoma (H), colon adenocarcinoma (I), breast invasive carcinoma of no special type (NOS; J), renal clear cell carcinoma (K), Ewing sarcoma (L), gastric adenocarcinoma (intestinal type; M), esophageal squamous cell carcinoma (N), and hepatocellular carcinoma (O). P, Representative RNA in situ hybridization performed in tissue sections probed by *Blm-s* riboprobe and immunodetected by AP with red chromogen. Shown in each left lower boxed area is hematoxylin-stained adjacent tissue section. Scale bar, 50 μm.

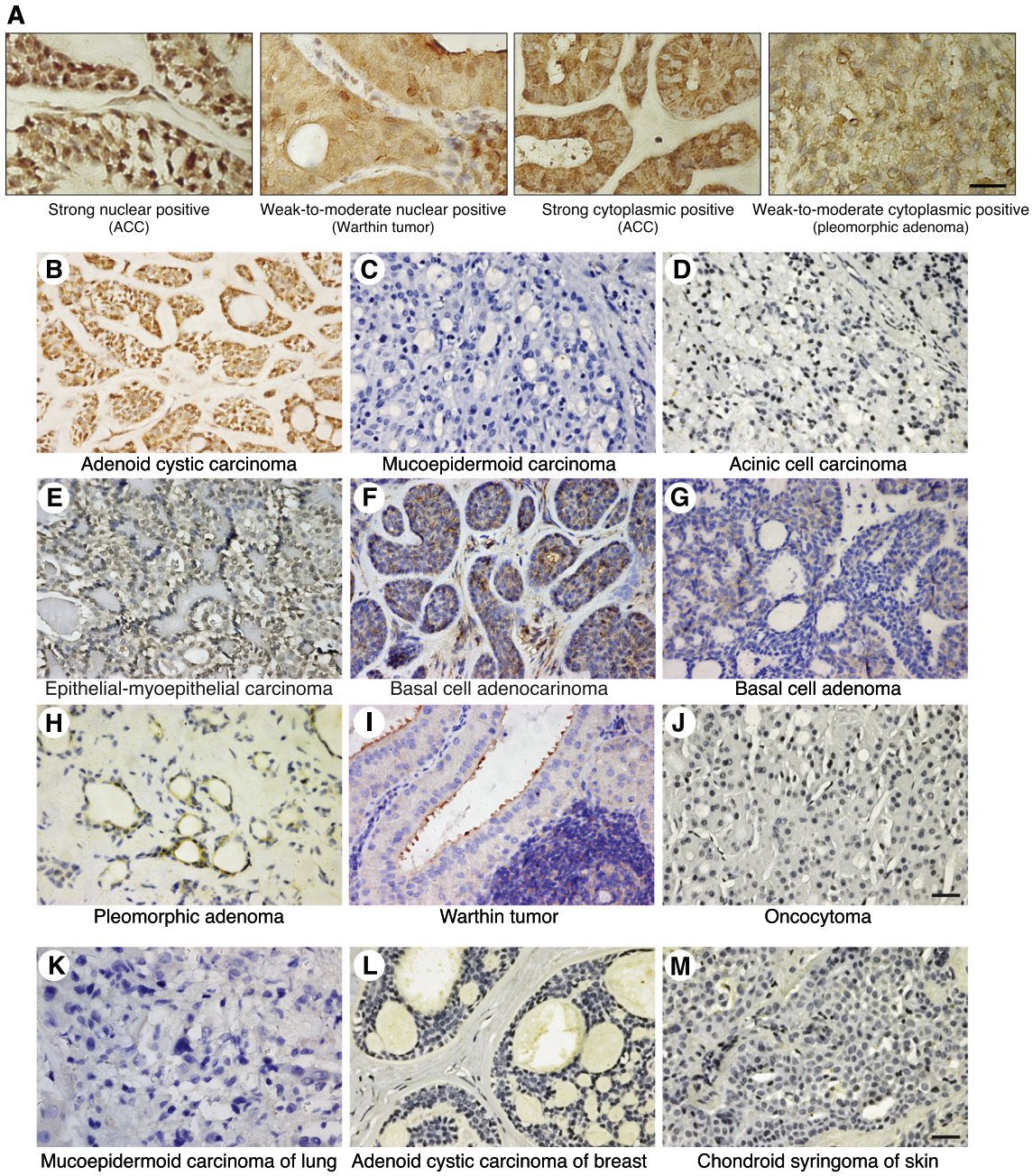

Fig. 3 Strong nuclear BLM-s immunoreactivity in ACC of salivary gland. A, Representative images for subcellular localization and immunointensity of BLM-s in salivary gland tumors. Immunohistochemistry of BLM-s in various subtypes of salivary gland tumors (B-J), pulmonary mucoepidermoid carcinoma (K), breast ACC (L), and skin chondroid syringoma (M). Noticeably, strong nuclear immunointensity of BLM-s in ACC derived from salivary gland (B) in comparison with negative BLM-s immunoreactivity in mucoepidermoid carcinoma derived from lung (K) or breast ACC (L). Scale bar, 50 μm.

2.4. Fluorescence in situ hybridization

Paraffin-embedded, 4-μm-thick sections were deparaffinized, rehydrated, and treated with protease K followed by commercially provided pretreatment buffer (Abbott Molecular, Des Plaines, IL, USA) at 80°C for 50 minutes. *MYB* Split FISH probes (Abnova, Taipei, Taiwan, ROC) or self-generated *MYBL1* FISH probes (RP11-707 M3: 3′ to *MYBL1* with green fluorescence; RP11-110 J18: 5′ to *MTBL1* with orange fluorescence) were applied to the pretreated sections. After being hybridized overnight at 4°C, sections were washed with TBS and counterstained with H33258. The slides were analyzed by scoring 100 nonoverlapping nuclei for each case independently by 2 pathologists using a fluorescence microscope (Zeiss, Oberkochen, Germany, AXIO Imager.D2) and AxioVision 4.5 software. Cases were considered to have *MYB* or

MYBL1 abnormality when at least 20% of the tumor cells harbored split signals that were at least 2-signal diameter apart.

2.5. Statistical analysis

The comparison of BLM-s expression between different salivary gland neoplasms was evaluated by SPSS 20 χ^2 test with post hoc *z* test (SPSS, Chicago, IL). Sensitivity and specificity of BLM-s immunohistochemistry among different types of tumor were performed by online software MedCalc, Ostend, Belgium (https://www.medcalc.org/calc/diagnostic_test.php), and the confidence intervals (CIs) of sensitivity and specificity are measured by Clopper-Pearson CIs. Statistical analysis of demographic characteristics of patients with ACC was performed using the Student *t* test for age and the Fisher exact test for sex, local recurrence, distant metastasis, and death.

3. Results

3.1. BLM-s is specifically expressed in salivary gland neoplasms

Several benign and malignant neoplasms paired with normal tissue (listed in Table 1) were used to perform BLM-s immunohistochemistry. The feasibility of using house-generated anti–BLM-s antibody for immunohistochemistry in human tissues is shown in Supplementary Fig. S1. For adult normal human tissues, BLM-s immunoreactivity was generally not detectable (Fig. 1D-O), except that the epithelia of the salivary striated ducts showed weak-to-moderate, cytoplasmic staining of BLM-s (Fig. 1A). Besides, BLM-s immunointensity was much enhanced in postirradiated ductal epithelia compared with those of normal salivary glands (Fig. 1B and C). It suggests that human homolog of BLM-s in salivary glands could be induced by DNA-damaging irradiation in a way much like what we have shown in murine brains [10].

In line with general null-BLM-s immunoreactivity in adult normal tissue, all non–salivary gland neoplasms had negative BLM-s immunoreactivity (Fig. 2C-O and Supplementary Fig. S2A-L). BLM-s immunoreactivity was only observed in tumors of salivary gland (see Table 1), as representatively shown in ACC (Fig. 2A) and mucoepidermoid carcinoma (Fig. 2B). Both cytoplasmic and nuclear expression patterns of BLM-s were observed in salivary gland tumors (Figs. 2A and B and 3A). Furthermore, via RNA in situ hybridization, we demonstrate that BLM-s transcripts were expressed in salivary gland tumors (Fig. 2P, left), which is in strong contrast to no signal in nonsalivary neoplasms, as representatively shown in colon adenocarcinoma (Fig. 2P, right). Regardless of the

Table 2 Subcellular pattern of BLM-s immunoreactivity in different subtypes of human salivary neoplasms

Diagnosis	Case no.	Negative, case no. (%)	Exclusively cytoplasmic positive, case no. (%)		Nuclear positive, case no. (%)	
			Weak-to-moderate	Strong	Weak-to-moderate	Strong
Warthin tumor	25	7 (28)	9 (36)	0 (0)	9 (36)**	0 (0)
Pleomorphic adenoma	26	5 (19)	21 (81)*	0 (0)	0 (0)	0 (0)
Oncocytoma	16	13 (81)	3 (19)	0 (0)	0 (0)	0 (0)
Myoepithelioma	12	9 (75)	3 (25)	0 (0)	0 (0)	0 (0)
Basal cell adenoma	21	10 (47.6)	11 (52.4)	0 (0)	0 (0)	0 (0)
Canalicular adenoma	1	0 (0)	1 (100)	0 (0)	0 (0)	0 (0)
Cystadenoma	9	5 (56)	3 (33)	1 (11)	0 (0)	0 (0)
Mucoepidermoid carcinoma	50	13 (26)	15 (30)	14 (28)*	2 (4)	6 (12)
ACC	38	5 (13)	9 (23.7)	3 (7.9)	0 (0)	21 (55.3)**
Acinic cell carcinoma	37	15 (41)	13 (35)	9 (24)*	0 (0)	0 (0)
Myoepithelial carcinoma	4	3 (75)	1 (25)	0 (0)	0 (0)	0 (0)
Basal cell adenocarcinoma	5	4 (80)	1 (20)	0 (0)	0 (0)	0 (0)
Epithelial-myoepithelial carcinoma	4	1 (25)	0 (0)	1 (25)	2 (50)**	0 (0)
Cystadenocarcinoma	2	1 (50)	1 (50)	0 (0)	0 (0)	0 (0)
Adenocarcinoma, not otherwise specified	7	3 (42.8)	2 (28.6)	2 (28.6)	0 (0)	0 (0)
Carcinoma ex pleomorphic adenoma	17	14 (82)	3 (18)	0 (0)	0 (0)	0 (0)
Salivary duct carcinoma	9	0 (0)	9 (100)*	0 (0)	0 (0)	0 (0)
Mammary analogue secretory carcinoma of salivary gland	4	0 (0)	4 (100)*	0 (0)	0 (0)	0 (0)
Squamous cell carcinoma	5	3 (60)	2 (40)	0 (0)	0 (0)	0 (0)
Small cell carcinoma	1	1 (100)	0 (0)	0 (0)	0 (0)	0 (0)
Lymphoepithelial carcinoma	5	2 (40)	3 (60)	0 (0)	0 (0)	0 (0)
Adenosquamous cell carcinoma	1	1 (100)	0 (0)	0 (0)	0 (0)	0 (0)

* $P < .05$, χ^2 post hoc test for cytoplasmic stain.
** $P < .05$, χ^2 post hoc test for nuclear stain.

differences in subcellular expression pattern, the specificity and sensitivity of positive-BLM-s immunoreactivity in correlation with salivary gland tumors, both benign and malignant included, are 0.76 (95% CI, 0.65-0.85) and 1 (95% CI, 0.99-1), respectively, in comparison with other non–salivary gland tumors. It suggests that detection of BLM-s expression in tumor cells is highly correlated with tumor origin derived from the salivary gland.

3.2. Nuclear expression of BLM-s is specifically observed in ACC originating from the salivary gland

Although BLM-s in normal salivary gland showed diffuse weak-to-moderate cytoplasmic staining pattern (Fig. 1A), nuclear expression pattern of BLM-s seemed to be the predominant feature observed in some subtypes of salivary gland tumors, especially for those diagnosed as ACC (Figs. 2A and 3B). To substantiate this observation, more cases with different tumor subtypes of salivary neoplasms were archived for BLM-s immunohistochemistry. We categorize BLM-s immunohistochemistry by its immunointensity and subcellular localization into 4 patterns: strong nuclear positive (with/without cytoplasmic staining), weak-to-moderate nuclear positive (with/without cytoplasmic staining), strong cytoplasmic positive exclusively (with no nuclear immunoreactivity), and weak-to-moderate cytoplasmic positive exclusively (Fig. 3A). As shown in Fig. 3 and Table 2, most salivary gland neoplasms had various degree of immunointensity for cytoplasmic BLM-s. Statistical analysis revealed that stronger cytoplasmic BLM-s staining tended to be more correlated with malignant nature of salivary gland tumors (22% versus 5%, $P < .001$, χ^2 test, with post hoc z test). By contrast, nuclear expression of BLM-s seemed to be observed only in few subtypes of salivary gland neoplasms, which include Warthin tumor, ACC, mucoepidermoid carcinoma, and epithelial-myoepithelial carcinoma (Table 2). Particularly, ACC had the highest percentage of nuclear BLM-s immunoreactivity (82%; versus mucoepidermoid carcinoma [16%] and epithelial-myoepithelial carcinoma [50%]) and had stronger nuclear-positivity of BLM-s (74%) in general (Fig. 2B and Table 2). The sensitivity and specificity of nuclear BLM-s immunoreactivity used to distinguish salivary ACC from other subtypes of salivary neoplasms are 0.82 (95% CI, 0.66-0.92) and 0.92 (95% CI, 0.88-0.95), respectively. Alternatively, comparison among various subtypes of malignant salivary gland neoplasms showed that the sensitivity and specificity of using nuclear BLM-s immunoreactivity to distinguish ACC from other tumors are 0.82 and 0.93 (95% CI, 0.87-0.97), respectively. Therefore, strong nuclear expression pattern of BLM-s immunohistochemistry is highly specific to salivary ACC.

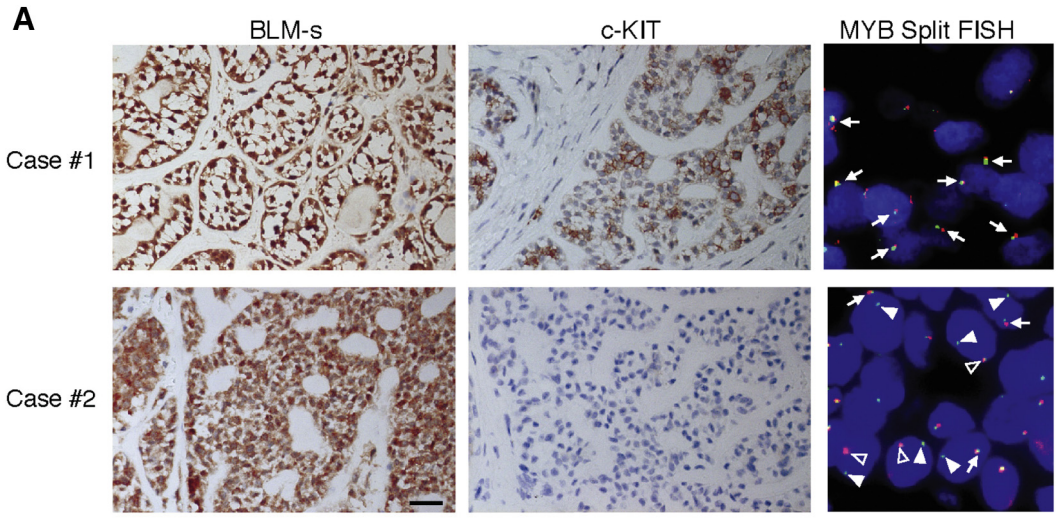

B

	False Negative rate	True Positive rate
Nuclear BLM-s IHC	18.5%	81.6%
c-KIT IHC	34.2%	65.8%
MYB (or MYBL1) FISH	26.3%	73.7%

Fig. 4 Comparison among BLM-s nuclear immunoreactivity, c-KIT immunohistochemistry, and *MYB* split FISH in salivary ACC. A, Representative salivary ACC cases with images of BLM-s immunohistochemistry, c-KIT immunohistochemistry, and *MYB* split FISH. White arrows, nonsplit *MYB* signal; arrowheads, split *MYB* signal; solid arrowhead, *MYB* (FITC, 780-kb probe; Abnova); empty, *MYB* (Texas Red, 500-kb probe; Abnova). Scale bar, 50 μm. B, Comparison of salivary ACC detection rate by each indicated method.

Table 3 BLM-s immunoreactivity, c-KIT immunohistochemistry, and *MYB/MYBL1* gene abnormality in subtypes of human salivary ACC

ACC subtype	Case no.	BLM-s					c-KIT, case no. (%)		*MYB* or *MYBL1* abnormality by FISH, case no. (%)	
		Negative, case no. (%)	Exclusively cytoplasmic positive, case no. (%)		Nuclear positive, case no. (%)					
			Weak-to-moderate	Strong	Weak-to-moderate	Strong	Negative	Positive	Negative	Positive
Cribriform	22 (58)	3 (13.6)	4 (18.2)	1 (4.5)	0 (0)	14 (63.6)	13 (59.1)	9 (40.9)	7 (31.8)	15 (63.2)
Tubular	8 (21)	0 (0)	2 (25)	1 (12.5)	0 (0)	5 (62.5)	0 (0)	8 (100)	2 (25.0)	6 (75.0)
Solid	8 (21)	2 (25.0)	3 (37.5)	1 (12.5)	0 (0)	2 (25.0)	0 (0)	8 (100)	3 (37.5)	5 (62.5)
Total	38	5 (13.2)	9 (23.7)	3 (7.9)	0 (0)	21 (55.3)	13 (34.2)	25 (65.8)	12 (31.6)	26 (68.4)

Similar morphologic characteristics of salivary ACC are also found in tumors of other tissue origin such as the breast. Besides, pulmonary mucoepidermoid carcinoma recapitulates morphologic characteristics of salivary mucoepidermoid carcinoma, some of which also expresses cytoplasmic or nuclear BLM-s. We thus wonder whether BLM-s is also expressed in these morphologically identical neoplasms of nonsalivary tissue origin. Because of rarity in mammary ACC and pulmonary mucoepidermoid carcinoma, we have obtained only 2 cases of pulmonary mucoepidermoid carcinoma and 3 cases of mammary ACC for BLM-s immunohistochemistry (including another 5 cases of skin chondroid syringoma for comparison). All of the cases are immunonegative for BLM-s (Fig. 3K-M). Therefore, nuclear expression pattern of BLM-s immunohistochemistry is highly specific for ACC originating from salivary gland.

3.3. Comparison among c-KIT immunohistochemistry, MYB/MYBL FISH, and BLM-s' nuclear immunoreactivity in salivary ACC

It has been shown that 50% to 60% of ACC overexpresses MYB resulting from recurrent balanced t(6:9)(q22-23;p23-24) translocation detected by FISH [19-23]. Besides, overexpression of c-KIT or EMT marker SNAIL/SLUG was reported to correlate with higher-grade ACC and poor prognosis [24-26]. Accordingly, we performed c-KIT immunohistochemistry, SNAIL/SLUG immunohistochemistry, and *MYB/MYBL1* FISH in our collected ACC cases (Fig. 4A and Supplementary Fig. S3) and compared the results with that from BLM-s immunohistochemistry. As shown in Table 3, there is no differential expression of BLM-s in ACC subtypes ($P = .73$, χ^2 test). Likewise, c-KIT immunostain, SNAIL immunohistochemistry, or *MYB/MYBL* FISH could not distinguish among ACC subtypes (Table 3 and Supplementary Table S1). Comparison of each method in correlation with ACC showed that positive BLM-s nuclear immunoreactivity is more correlated with ACC than other methods, resulting in less false-negative (18.5% versus 34.2% and 26.3%) and higher true-positive detection rate (81.6% versus 65.8% and 73.7%) of ACC (Fig. 4B).

3.4. Study of demographic correlation with BLM-s expression pattern in salivary ACC

We also examine a possible correlation of nuclear-expressed BLM-s with any demographic characteristic in salivary ACC. Because of lost follow-up of some patients, only 30 of our collected 38 cases with salivary ACC were available for analysis. As shown in Table 4, BLM-s–positive and BLM-s–negative patient groups showed no statistical difference in age and sex. Local recurrence seemed to be detected only in BLM-s–positive groups, although statistical analysis did not reveal significance ($P = .798$). The disease-free survival rate is not statistically significant ($P = .265$, log-rank test of Kaplan-Meier estimator), given that local recurrence and/or

Table 4 Statistical correlation between BLM-s expression pattern and each clinical characteristic in 30 patients with salivary ACC

	Age (y)	Sex (male/female)	Local recurrence	Distant metastasis	Death
BLM-s (−)	60 ± 19.8	2/2	0	0	0
BLM-s (+)					
Cytoplasmic	58 ± 16.8	3/5	1	2	1
Nuclear	49 ± 17.6	4/10	1	0	0
Cytoplasmic and nuclear	59 ± 16.4	0/4	0	2	1
P	.665	.397	1.000	.018	.202

NOTE. *P* value for age is derived using the Student *t* test, and *P* for others are derived using the Fisher exact test.

distant metastasis developed only in 4 of the 30 patients. Given that most salivary gland malignancies are not lethal by their biological nature and that only 2 of the 30 patients in this study died of ACC, the overall survival rate followed for up to 10 years was hard to be interpreted properly ($P = .255$, log-rank test of Kaplan-Meier estimator).

4. Discussion

Diagnosis of salivary neoplasms by fine-needle aspiration/biopsy in the head and neck regions is challenging because of high false-negative result [27]. Particularly, the histologic feature of ACC simulates other basal cell neoplasms, necessitating the development of ancillary immunohistochemistry or molecular tools. It has been reported that MYB is immunohistochemically detectable in most ACCs and could be used to distinguish ACC from MYB-negative pleomorphic adenoma in fine-needle aspiration biopsy specimen [28]. More recently, recurrent balanced t(6;9)(q22-23;p23-24) translocation that results in overexpressed *MYB-NFIB*–fused transcript and protein is reported in 50% to 60% of ACC detected by FISH and in 38.2% of ACC detected by immunohistochemistry [20-24]. However, *MYB-NFIB* fusion gene is also detected in mammary ACC such that *MYB-NFIB*–fused transcript could not be used as a signature for salivary ACC. Another candidate molecule as a diagnostic marker of salivary ACC is the receptor tyrosine kinase c-KIT, which is uncovered as one of the frequently mutated genes by whole genome or exome sequencing [29,30]. Although c-KIT overexpression is reported to correlate with grade 3 ACC and with poor prognosis, usage of c-KIT expression as a diagnostic marker of salivary ACC is questionable because its expression level has not been fully examined in other subtypes of salivary gland tumors [31]. In addition, the specificity of usage of c-KIT expression to diagnose salivary ACC is compromised because other tumors such as triple-negative breast ACCs also express c-KIT [32]. Here, our study suggests that nuclear BLM-s immunoreactivity could potentially serve as an ancillary diagnostic tool for ACC originating from the salivary gland, even when the tissue size of the tumor is small (Supplementary Fig. S4).

Nuclear localization of BLM-s in salivary ACC is quite unique, given that BLM-s usually localizes in the mitochondria and endoplasmic reticulum to function as a proapoptotic molecule [10]. Because BCL-2 family member executes cell death depending much on its subcellular localization, aberrant localization of BCL-2 family is a common strategy used by cancer cells to escape apoptosis. For example, ectopic nuclear localization of proapoptotic BAX is frequently reported in lung cancer [33] and colorectal cancer [34]. We thus suspect that aberrant BLM-s localization in the nucleus of salivary ACC tumor cells might render tumor cells more resistant to apoptosis.

Whole genome and exome sequencing of ACC reveals that increased ATM kinase activity in DNA damage repair pathway through missense mutation in *ATM* gene is one of the major mechanisms underlying salivary ACC tumorigenesis [29,30]. Intriguingly, BLM-s gene is one of the target genes downstream of ATM/p53 signaling in response to DNA damage [10]. Besides, stronger BLM-s immunoreactivity in postirradiated human salivary glands (Fig. 1B and C) also suggests induction of BLM-s by DNA-damage signaling pathways in salivary glands. Accordingly, we suspect that overexpression of BLM-s in salivary ACC might be partly attributed to activating mutation of *ATM* during ACC tumorigenesis. Noticeably, ACC overexpresses other BCL-2 family members including the prosurvival BCL-2 and BCL-x_L [35], which are the target genes of MYB [36]. Therefore, aberrant expression of the BCL-2 family members in salivary ACC is a common readout as being downstream targets of key mutator genes such as *ATM* and *MYB* genes during ACC tumorigenesis.

Supplementary data

Supplementary data to this article can be found online at https://doi.org/10.1016/j.humpath.2018.09.005.

Author contributions

Tsai M. S. and Huang P. H. conceived and designed the experiments. Tsai M. S., Hsieh M. S., and Huang H. Y. performed the experiments. Tsai M. S., Hsieh M. S., Huang H. Y., and Huang P. H. analyzed the data. Tsai M. S. and Huang P. H. wrote the manuscript.

References

[1] Kiraz Y, Adan A, Kartal Yandim M, Baran Y. Major apoptotic mechanisms and genes involved in apoptosis. Tumour Biol 2016;37:8471-86.
[2] Fernald K, Kurokawa M. Evading apoptosis in cancer. Trends Cell Biol 2013;23:620-33.
[3] Choi J, Choi K, Benveniste EN, et al. Bcl-2 promotes invasion and lung metastasis by inducing matrix metalloproteinase-2. Cancer Res 2005;65:5554-60.
[4] Wick W, Wagner S, Kerkau S, Dichgans J, Tonn JC, Weller M. BCL-2 promotes migration and invasiveness of human glioma cells. FEBS Lett 1998;440:419-24.
[5] Perego P, Giarola M, Righetti SC, et al. Association between cisplatin resistance and mutation of p53 gene and reduced bax expression in ovarian carcinoma cell systems. Cancer Res 1996;56:556-62.
[6] Johnson MI, Robinson MC, Marsh C, Robson CN, Neal DE, Hamdy FC. Expression of Bcl-2, Bax, and p53 in high-grade prostatic intraepithelial neoplasia and localized prostate cancer: relationship with apoptosis and proliferation. Prostate 1998;37:223-9.
[7] Meijerink JP, Mensink EJ, Wang K, et al. Hematopoietic malignancies demonstrate loss-of-function mutations of BAX. Blood 1998;91:2991-7.
[8] Tagawa H, Karnan S, Suzuki R, et al. Genome-wide array-based CGH for mantle cell lymphoma: identification of homozygous deletions of the proapoptotic gene BIM. Oncogene 2005;24:1348-58.

[9] Zantl N, Weirich G, Zall H, et al. Frequent loss of expression of the pro-apoptotic protein Bim in renal cell carcinoma: evidence for contribution to apoptosis resistance. Oncogene 2007;26:7038-48.
[10] Liu WW, Chen SY, Cheng CH, Cheng HJ, Huang PH. Blm-s, a BH3-only protein enriched in postmitotic immature neurons, is transcriptionally upregulated by p53 during DNA damage. Cell Rep 2014;9:166-79.
[11] Paquin N, Murata Y, Froehlich A, et al. The conserved VPS-50 protein functions in dense core vesicle maturation and acidification and controls animal behavior. Curr Biol 2016;26:862-71.
[12] Schindler C, Chen Y, Pu J, Guo X, Bonifacino JS. EARP is a multisubunit tethering complex involved in endocytic recylcing. Nat Cell Biol 2015;17:639-50.
[13] Gillingham AK, Sinka R, Torres IL, Lilley KS, Munro S. Towards a comprehensive map of the effectors of Rab GTPases. Dev Cell 2014; 31:358-73.
[14] Matsumoto Y, Imai Y, Sugita Y, et al. CCDC132 is highly expressed in atopic dermatitis T cells. Mol Med Rep 2010;3:83-7.
[15] Ellington CL, Goodman M, Kono SA, et al. Adenoid cystic carcinoma of the head and neck: incidence and survival trends based on 1973-2007 surveillance, epidemiology, and end results data. Cancer 2012;118:4444-51.
[16] Coca-Pelaz A, Rodrigo JP, Bradley PJ, et al. Adenoid cystic carcinoma of the head and neck—an update. Oral Oncol 2015;51:652-61.
[17] Skálová A, Stenman G, Simpson RH, et al. The role of molecular testing in the differential diagnosis of salivary gland carcinomas. Am J Surg Pathol 2018;42:e11-27.
[18] Tseng CH, Murray KD, Jou MF, Hsu SM, Cheng HJ, Huang PH. Sema3E/plexin-D1 mediated epithelial-to-mesenchymal transition in ovarian endometrioid cancer. PLoS One 2011;6:e19396.
[19] Persson M, Andrén Y, Mark J, Horlings HM, Persson F, Stenman G. Recurrent fusion of MYB and NFIB transcription factor genes in carcinomas of the breast and head and neck. Proc Natl Acad Sci U S A 2009; 106:18740-4.
[20] Mitani Y, Li J, Rao PH, et al. Comprehensive analysis of the MYB-NFIB gene fusion in salivary adenoid cystic carcinoma: incidence, variability, and clinicopathologic significance. Clin Cancer Res 2010;16:4722-31.
[21] Mitani Y, Rao PH, Futreal PA, et al. Novel chromosomal rearrangements and break points at the t(6;9) in salivary adenoid cystic carcinoma: association with MYB-NFIB chimeric fusion, MYB expression, and clinical outcome. Clin Cancer Res 2011;17:7003-14.
[22] West RB, Kong C, Clarke N, et al. MYB expression and translocation in adenoid cystic carcinomas and other salivary gland tumors with clinicopathologic correlation. Am J Surg Pathol 2011;35:92-9.
[23] Mitani Y, Liu B, Rao PH, et al. Novel MYBL1 gene rearrangements with recurrent MYBL1-NFIB fusions in salivary adenoid cystic carcinomas lacking t(6;9) translocations. Clin Cancer Res 2016;22:725-33.
[24] Holst VA, Marshall CE, Moskaluk CA, Frierson Jr HF. KIT protein expression and analysis of c-kit gene mutation in adenoid cystic carcinoma. Mod Pathol 1999;12:956-60.
[25] Phuchareon J, van Zante A, Overdevest JB, McCormick F, Eisele DW, Tetsu O. c-Kit expression is rate-limiting for stem cell factor–mediated disease progression in adenoid cystic carcinoma of the salivary glands. Transl Oncol 2014;7:537-45.
[26] Tang Y, Liang X, Zheng M, et al. Expression of c-Kit and Slug correlates with invasion and metastasis of salivary adenoid cystic carcinoma. Oral Oncol 2010;46:311-6.
[27] Daneshbod Y, Daneshbod K, Khademi B. Diagnostic difficulties in the interpretation of fine needle aspirate samples in salivary lesions: diagnostic pitfalls revisited. Acta Cytol 2009;53:53-70.
[28] Pusztaszeri MP, Faquin WC. MYB is a helpful diagnostic marker for adenoid cystic carcinoma in fine-needle aspiration biopsy. Arch Pathol Lab Med 2015;139:157-8.
[29] Stephens PJ, Davies HR, Mitani Y, et al. Whole exome sequencing of adenoid cystic carcinoma. J Clin Invest 2013;123:2965-8.
[30] Ho AS, Kannan K, Roy DM, et al. The mutational landscape of adenoid cystic carcinoma. Nat Genet 2013;45:791-8.
[31] Mino M, Pilch BZ, Faquin WC. Expression of KIT (CD117) in neoplasms of the head and neck: an ancillary marker for adenoid cystic carcinoma. Mod Pathol 2003;16:1224-31.
[32] Azoulay S, Lae M, Freneaux P, et al. KIT is highly expressed in adenoid cystic carcinoma of the breast, a basal-like carcinoma associated with a favorable outcome. Mod Pathol 2005;18:1623-31.
[33] Salah-eldin A, Inoue S, Tsuda M, Matsuura A. Abnormal intracellular localization of Bax with a normal membrane anchor domain in human lung cancer cell lines. Jpn J Cancer Res 2000;91:1269-77.
[34] Mandal M, Adam L, Mendelsohn J, Kumar R. Nuclear targeting of Bax during apoptosis in human colorectal cancer cells. Oncogene 1998;17: 999-1007.
[35] Carlinfante G, Lazzaretti M, Ferrari S, Bianchi B, Crafa P. P53, bcl-2 and Ki-67 expression in adenoid cystic carcinoma of the palate. A clinicopathologic study of 21 cases with long-term follow-up. Pathol Res Pract 2005;200:791-9.
[36] Bell D, Roberts D, Karpowicz M, Hanna EY, Weber RS, El-Naggar AK. Clinical significance of Myb protein and downstream target genes in salivary adenoid cystic carcinoma. Cancer Biol Ther 2011;12:569-73.